

Comparison of Four Cloud Schemes in Simulating the Seasonal Mean field forced by
the Observed Sea Surface Temperature

Akihiko Shimpo*, Masao Kanamitsu, Sam F. Iacobellis

Scripps Institution of Oceanography, University of California, San Diego, La Jolla, California

Song-You Hong

Global Environment Laboratory, Department of Atmospheric Sciences,

Yonsei University, Seoul, South Korea

Submitted to Monthly Weather Review

Revised June 28, 2007

*On leave from Climate Prediction Division, Japan Meteorological Agency

Corresponding Author: Akihiko Shimpo, Climate Prediction Division, Japan Meteorological
Agency, Tokyo, Japan

Email: ashimpo@naps.kishou.go.jp

ABSTRACT

The impacts of four stratiform cloud parameterizations on seasonal mean fields are investigated using the global version of the Experimental Climate Prediction Center (ECPC) global to regional forecast system (G-RSM). The simulated fields are compared with observation and reanalysis, including the International Satellite Cloud Climatology Project (ISCCP) data for clouds, the Global Precipitation Climatology Project (GPCP) data for precipitation, the Earth Radiation Budget Experiment (ERBE) and the Surface Radiation Budget Project (SRB) data for radiation and the NCEP / Department of Energy (DOE) Reanalysis-2 (R-2) for temperature.

Compared to observation, no stratiform cloud parameterization performed better than others in all respects in simulating clouds, temperature, precipitation and radiation fluxes. This result may be caused by the fact that no fine tuning was performed to improve simulation for each stratiform cloud parameterization, together with the fact that the simulation is very sensitive to some of the key parameters in each parameterization. It is also found that there is a strong interaction between parameterized stratiform clouds with boundary layer clouds and convection, resulted in the change in the simulation of low level cloudiness and precipitation.

When the simulations are compared with ISCCP cloudiness and cloud water, and the NCEP/DOE R-2 relative humidity, it is found that the cloud amount depends mostly on the relative humidity with less dependency on model cloud water, while the cloud amount is more strongly dependent on cloud water than relative humidity in the satellite observations. From these results, a new cloudiness formula based only on cloud water is proposed. When the new scheme is tested using independent satellite observed cloud water, it provides better cloud amount distribution than cloud schemes dependent on relative humidity. However, the

application of this new cloud scheme to model simulation is limited since the error and bias of the simulated cloud water are large and the cloud distribution directly reflects these errors.

1. Introduction

Clouds are one of the most uncertain components in climate models and model results are known to be very sensitive to cloud parameterizations. The accurate simulation of cloud amount, vertical distribution, and the radiative property of clouds are particularly important for ocean atmosphere coupling due to the large impact of clouds on short and long wave radiation fluxes reaching the ocean.

To improve the simulation of cloud amount¹, several cloudiness parameterizations for stratiform clouds have been proposed, which can be divided into the following three types. The first is based on the probability density function (PDF) of the subgrid-scale distribution of total water (sum of specific humidity and cloud water) and cloud amount is determined from the ratio between specific humidity and cloud water (e.g. Smith 1990; Lohmann et al. 1999; Rotstayn et al. 2000; Tompkins 2002). In the second type, cloud amount is diagnosed from relative humidity (e.g. Slingo 1987; Slingo and Slingo 1991) or from both relative humidity and cloud water (e.g. Randall 1995; Xu and Randall 1996). In the third type, cloud amount is predicted as a new predictive variable using an equation considering source and sink of cloud amount (e.g. Tiedtke

¹ In numerical weather prediction (NWP) models and general circulation models (GCMs), the portion of precipitation from a microphysical process and its precipitation processes is regarded as grid-resolvable precipitation, and the parameterized processes from the cumulus parameterization scheme is regarded as sub-grid scale precipitation. In this study, the cloudiness and precipitation from the grid-resolvable precipitation algorithm are defined by stratiform clouds and large-scale precipitation, whereas they are termed as convective clouds and convective precipitation for the portion of the cumulus parameterization scheme.

1993). There are other types of cloudiness parameterization, particularly for convective clouds (Bony and Emanuel 2001) and boundary layer clouds (e.g. Teixeira and Hogan 2002; Bretherton et al. 2004a). Some of the formulations are based on theoretical consideration, while others are more empirically derived from observational data. In addition, many of the schemes are based on Cloud Resolving Model (CRM) and Large Eddy Simulation (LES) model forced by observational data (e.g. Randall 1995; Xu and Randall 1996).

These cloud parameterizations have been used in both operational NWP models and GCMs. For example, in the Hadley Centre coupled model (HadCM3), the large-scale precipitation and cloud scheme (Gordon et al. 2000) is formulated following Smith (1990), which is the PDF type. The Japan Meteorological Agency Global Spectral Model (JMA GSM) adopts the PDF type cloud scheme based on Sommeria and Deardorff (1977) similar to Smith's formula but its microphysics is based on Sundqvist (1978) and Sundqvist et al. (1989). The NCEP Global Forecast System (GFS) and Climate Forecast System (CFS) models have one cloud condensate as a prognostic variable (Sundqvist et al. 1989; Zhao and Carr 1997) and cloud amount is diagnosed from relative humidity and cloud condensate based on Xu and Randall (1996). In the ECMWF Integrated Forecast System (IFS), not only cloud condensate but also cloud amount is predicted following Tiedtke (1993). For the cloud water, only single cloud condensate is incorporated as a prognostic variable in some models, while others have separate prognostic equations for cloud water and ice. The NCAR Community Atmosphere Model version 3 (CAM3: Collins et al. 2006) included both the prognostic cloud water and ice equations (Boville et al. 2006), however, stratiform cloud amount is diagnosed from relative humidity only. The GFDL global atmosphere model (AM2: the GFDL Global Atmospheric Model Development Team 2004; Delworth et al. 2006) included both cloud water and ice

separately (Rotstayn et al. 2000), and cloud amount as prognostic variables based on Tiedtke (1993).

The efforts to improve cloud representation in models have improved weather forecasts and climate simulations. For example, Tiedtke (1993) showed that their prognostic cloud scheme produced realistic cloud fields compared to observed cloud cover and cloud water content, and improved the forecasts skill of the ECMWF global model. Fowler et al. (1996) implemented a more sophisticated prognostic cloud scheme in the Colorado State University (CSU) GCM and showed improved cloud-radiation feedback. Boville et al. (2006) showed the predicted tropical tropopause temperature was greatly improved in CAM3, due to a better representation of cloud ice near the tropopause.

Another major advantage of using prognostic equations for the cloud condensates is that cloud driven radiation processes can be treated more physically without referring to the statistics based on the present-day atmosphere. This is very important when comparing the simulated current and future climates. Senior and Mitchell (1993) found that the presence or absence of cloud microphysical and optical thickness feedbacks could cause the global warming of the surface temperature to range from 1.9°C to 5.4°C in their doubled CO₂ experiments if different cloud parameterizations are used in a GCM.

In order to identify the importance of cloud representation, we will compare cloud water parameterizations and cloud parameterizations incorporated into the Experimental Climate Prediction Center (ECPC) global to regional forecast system (G-RSM) in simulations forced by the observed SSTs. Using a single GCM has the advantage of avoiding the effects of differences in other physics and dynamics, and of showing the impact of cloud parameterization more clearly. We will pay particular attention to the cloud parameterizations associated with stratiform clouds,

including three conceptually different prognostic cloud water schemes. It is expected that this study helps clarify the uncertainty of cloud simulations in different GCMs and global operational models.

The scope of this paper is limited to the impact of different cloud parameterizations on seasonal mean field. We do not examine the model skill, since transient and inter-annual behavior of the simulation requires long ensemble integrations of the order of 50 or more years for statistically meaningful results and we simply do not have sufficient resources to perform such integrations. We realize that the impact of parameterization on transient behavior, such as simulation of interannual variability, is very different from what is expected from seasonal mean behavior.

This paper is organized as follows. In section 2, the cloud parameterizations used in this study are presented. The observation and reanalysis data, model and experimental setup are given in Section 3. In section 4, experimental results using each cloud scheme are shown. In section 5, relationships between relative humidity, cloud amount and cloud water are discussed. Conclusions are presented in section 6.

2. Cloud parameterizations examined in this study

The comparison of cloudiness parameterizations in the model is not straightforward due to the separation of cloudiness into three distinctly different types; 1) stratiform cloud, 2) convective cloud and 3) inversion topped boundary layer cloud. These three types of clouds are treated independently in most models. We realize that there may be a strong interaction between these different types of cloudiness; however, it is beyond our resources to perform a combination of all the different types of parameterizations. Knowing these restrictions, and confining our interest to the cloud associated with stratiform cloud, we tried to apply the same cloudiness

parameterizations for convective cloud and inversion topped boundary layer cloud whenever possible. The summary of the combination of these three types of cloud parameterizations examined in this study is shown in Table.1

Before explaining the detail of the stratiform cloudiness parameterizations examined in this study, we will explain the cloudiness associated with convective cloud and inversion topped boundary layer cloud first.

2.1 Cloudiness associated with convective cloud

Cloudiness associated with convective cloud in most of the schemes, except Iacobellis and Somerville (section 2.3.3), is based on Slingo (1987). The convective cloud amount (C_c) is based on the convective precipitation rate (P_{cnv}) from the model's convection scheme using the following empirical relationship:

$$C_c = 0.200 + 0.120 \ln P_{cnv}, \quad (1)$$

the coefficients in the formula above were adjusted to fit observed cloudiness.

In addition, for the Slingo scheme (Section 2.3.1), anvil cirrus is assumed to form if $C_c \geq 0.3$ and the cloud top is higher than $\sigma = 0.4$, where σ is the vertical coordinate of the model (400 hPa when the surface pressure is 1000 hPa). The cloud bases and tops are determined by the mass flux vertical distribution in the convective parameterization. The cloud amount (C) due to anvil cirrus in the model layer is calculated as

$$C = 2(C_c - 0.3), \quad (2)$$

For the schemes with cloud water as a predictive variable, this somewhat artificial increase in upper level cloudiness is turned off, and the detrainment of cloud water from the top of the convective cloud is added as a source of cloud water in the cloud water prediction equation. By doing so, the cloudiness calculation is left to the stratiform cloudiness

parameterization

2.2 Cloudiness associated with inversion topped boundary layer cloud (marine stratus)

The stratus over cold ocean topped by strong atmospheric inversion is prevalent over the eastern Pacific and Atlantic (e.g. Bretherton et al. 2004b). This type of cloud, commonly called marine stratus, is extremely important for atmospheric and ocean interaction, but very difficult to simulate by the cloud physical processes currently incorporated into the numerical models (e.g. Stevens et al. 2001, 2005; Duynkerke and Teixeira 2001; Bretherton et al. 2004a). Therefore, this type of cloud is parameterized independently using empirical means. The scheme used in this study is taken from Slingo (1987). When there is subsidence ($\omega \geq 0$) over ocean below 870 hPa, and if an inversion is present with $\partial\theta/\partial p \leq -0.055 \text{ K hPa}^{-1}$, the scheme assumes that there is an inversion topped boundary layer cloud. The cloud amount is determined from the inversion intensity and relative humidity RH_B at the inversion base:

$$\begin{aligned}
 C &= 0, & \text{for } RH_B < 0.55 \\
 C &= \left(-16.67 \frac{\partial\theta}{\partial p} - 0.92 \right) \left(\frac{RH_B - 0.55}{0.25} \right), & \text{for } 0.55 \leq RH_B \leq 0.80 \quad (3) \\
 C &= \left(-16.67 \frac{\partial\theta}{\partial p} - 0.92 \right), & \text{for } RH_B > 0.80
 \end{aligned}$$

This parameterization is used in all the experiments performed in this study. We found that the marine stratus coverage, and accordingly the low level cloud coverage are very sensitive to the choice of the specification of the allowable top of the boundary layer (870 hPa, in this study). For the purpose of comparing various stratiform clouds, we intentionally left this parameter alone without adjusting it to make the simulation fit better with observations.

2.3 Cloudiness associated with stratiform cloud

All the schemes except the Slingo scheme (Section 2.3.1), utilize cloud water to

determine cloudiness, and therefore some detail of the cloud water prediction is also given.

2.3.1 Relative humidity-based scheme (Slingo scheme)

In the control simulation (SLINGO), the calculation of cloud amount is based on Slingo (1987). The stratiform cloud amount is calculated as

$$C = \begin{cases} \left(\frac{RH - RH_c}{1 - RH_c} \right)^2, & \text{for } RH > RH_c \\ 0, & \text{for } RH \leq RH_c \end{cases} \quad (4)$$

where RH is the mean relative humidity over the area represented by a grid, RH_c is the critical value of relative humidity for the cloud to form, which is calculated for each three layered cloud, high, middle and low, from historical forecast and corresponding observation to fit observed cloudiness. In this study, 0.85, 0.65, 0.85, 0.90, and 0.70 are used for high cloud over both land and ocean, middle cloud over land, middle cloud over ocean, low cloud over land and low cloud over ocean. Relative humidity is calculated with respect to water for all range of temperatures.

In radiation calculation, cloud optical properties are derived as a function of the cloud water path (CWP), which is assumed to be simply a function of temperature (Slingo 1989). Supersaturation is removed instantaneously as precipitation and evaporation occurs when precipitation falls through the unsaturated atmospheric layers.

2.3.2 Zhao and Carr's cloud water scheme (ZC)

The simplest prognostic cloud water scheme used in this study is based Zhao and Carr (1997), originated from Sundqvist et al. (1989). The prediction equation for cloud water/ice mixing ratio is

$$\frac{\partial q_c}{\partial t} = A(q_c) + S_c + S_g - P - E_c + D_{q_c}, \quad (5)$$

where q_c is the cloud water/ice mixing ratio, $A(q_c)$ is the horizontal advection of q_c , S_c and S_g are

the sources of q_c from convection (sub-grid scale) and stratiform (grid scale) clouds, respectively. P is the precipitation production rate from the cloud water/ice mixing ratio, E_c is the cloud evaporation rate, and D_{qc} is the horizontal and vertical diffusion. S_c is calculated from the detrainment of cloud water from the top of the convective cloud through the convective parameterization. S_g is a function of the tendencies of specific humidity, temperature and pressure. Since ice effect is considered, relative humidity is calculated with respect to water in cloud water regions and with respect to ice in cloud ice regions. The distinction between cloud water and ice is based on the temperature (T) in the simulation. In the regions where $T > 0^\circ\text{C}$, there is no cloud ice and relative humidity is calculated with respect to water, while in regions where $T < -15^\circ\text{C}$, no cloud water is allowed and relative humidity is calculated with respect to ice. In the regions where T is between -15°C and 0°C , clouds are estimated either cloud water or cloud ice. If there are cloud ice particles above this point at the previous or current time step, or if the cloud at this point at the previous time step consists of ice particles, then the hydrometeor at this point is ice particles and relative humidity is calculated with respect to ice. Otherwise, all clouds in this region are considered to contain supercooled cloud water and relative humidity is calculated with respect to water. To calculate precipitation production rate P , autoconversion of cloud water/ice to rain/snow, correction of cloud substance by falling precipitation, and melting of snow below the freezing level are taken into account. Here, the equations of autoconversion schemes are shown. The autoconversion of cloud water to rain is parameterized following Sundqvist et al. (1989) as

$$P_{\text{raut}} = c_0 q_c \left\{ 1 - \exp \left[- \left(\frac{q_c}{q_{cr} b} \right)^2 \right] \right\}, \quad (6)$$

where constants c_0 and q_{cr} are $1.0 \times 10^{-4} \text{ s}^{-1}$ and $3.0 \times 10^{-4} (\text{kg kg}^{-1})$, respectively. Cloud

coverage b is calculated using the equation (Sundqvist et al. 1989)

$$b = 1 - \left(\frac{1 - RH}{1 - RH_b} \right) \quad (7)$$

In this paper, RH_b is set to 0.85 for all grids based on sensitivity studies. The autoconversion of cloud ice to snow is parameterized following Lin et al. (1983) as

$$P_{saut} = a_1 (q_c - q_{ci0}), \quad (8)$$

where q_{ci0} is the threshold of cloud ice to snow and is set to a value of 5.0×10^{-6} (kg kg^{-1}), which is smaller value compared to the original paper. a_1 is specified as a function of temperature to take into account the temperature effect on P_{saut} .

In radiation calculation, cloud amount is calculated using Randall's (1995) formula:

$$C = RH \left[1 - \exp \left(\frac{-\alpha q_c}{1 - RH} \right) \right], \quad (9)$$

where constant α is 1000. Relative humidity in the regions where $T > 0^\circ\text{C}$ is calculated with respect to water, while it is calculated with respect to ice in the regions where $T < 0^\circ\text{C}$. It should be noted that there is inconsistency in the treatment of ice effect between the cloud water scheme and radiation scheme when ZC scheme is used in the simulation. Radiative properties of clouds are calculated using cloud water content. Cloud optical properties are calculated as a function of the CWP using the parameterization by Slingo (1989) for liquid water clouds, and Ebert and Curry (1992) for ice clouds. The effective cloud droplet radius for liquid water cloud is parameterized following Wyser (1998), and for ice cloud following Bower et al. (1994). This scheme is used in both medium range and seasonal operational forecast at the NCEP.

2.3.3 Iacobellis and Somerville's cloud scheme (IS)

The Iacobellis and Somerville cloud scheme (Iacobellis and Somerville 2000),

originated from Tiedtke (1993), predicts both the cloud water/ice mixing ratio and cloud amount.

The prediction equation for the cloud water/ice mixing ratio is

$$\frac{\partial q_c}{\partial t} = A(q_c) + S_c + S_{BL} + S_g - P - E_c + D_{q_c}, \quad (10)$$

where S_{BL} is the source of cloud water/ice from boundary-layer turbulence. S_c is calculated from the detrainment of cloud water from the top of the convective cloud through the convective parameterization. To calculate S_g , in the IS scheme based on Tiedtke (1993), tendency of saturation specific humidity affected by large-scale lifting and diabatic cooling is taken into account. S_{BL} , which is not included in the ZC scheme, is calculated through the turbulent moisture transport estimated in the boundary layer scheme. Relative humidity in the regions where $T > 0^\circ\text{C}$ is calculated with respect to water, while it is calculated with respect to ice in the regions where $T < 0^\circ\text{C}$. Precipitation processes for both cloud water and ice are represented following Sundqvist et al. (1989), similar to Eq. (6), however, c_0 and q_{cr} are not constants to take into account the effect of collection of cloud droplets by raindrops falling through the cloud, the Bergeron-Findeisen process, and the case of cirrus clouds. In addition, predicted cloud amount, which is described next, is used as b in (6).

For cloud amount, the prediction equation is

$$\frac{\partial C}{\partial t} = A(C) + S(C)_c + S(C)_{BL} + S(C)_g - D(C), \quad (11)$$

where $A(C)$ is the horizontal advection of clouds, $S(C)_c$, $S(C)_{BL}$, and $S(C)_g$ are the formation of cloud area by convection, boundary-layer turbulence, and stratiform condensation processes, respectively, and $D(C)$ is the rate of evaporation of clouds. Cloud radiative properties are calculated using the same parameterizations as ZC.

2.3.4 Hong's cloud water schemes (HONG)

Hong's cloud schemes (HONG_n, 'n' being the number of predicted water substance including water vapor) formulate clouds and precipitation as a bulk type as done in Lin et al. (1983), Rutledge and Hobbs (1983) and Dudhia (1989), but incorporate improved ice process treatment (Hong et al. 2004). In this study, three water substance prediction scheme is used due to its highest efficiency.

The scheme has a rain/snow mixing ratio in addition to a cloud water/ice mixing ratio as prognostic variables. The model prediction equation for the cloud water/ice mixing ratio and rain/snow mixing ratio are

$$\begin{aligned}\frac{\partial q_c}{\partial t} &= A(q_c) + F(q_c) + D_{qc}, \\ \frac{\partial q_r}{\partial t} &= A(q_r) + F(q_r) + D_{qr} - P,\end{aligned}\tag{12}$$

where q_r is the rain/snow mixing ratio, D_{qr} is the horizontal and vertical diffusion of q_r , and P is the sedimentation of falling precipitation drops. Though the microphysical processes in this scheme represent only the single term $F(q_c)$ and $F(q_r)$ for the cloud water/ice mixing ratio and rain/snow mixing ratio, respectively, they contain condensation of water vapor into cloud water and ice at saturation, accretion of cloud by rain and ice by snow, evaporation and sublimation of rain and snow, initiation and sedimentation of ice crystals and sublimation or deposition of ice crystals. Relative humidity in the regions where $T > 0^\circ\text{C}$ is calculated with respect to water, while it is calculated with respect to ice in the regions where $T < 0^\circ\text{C}$. About the precipitation production, the autoconversion of cloud water to rain is parameterized following Kessler (1969) as

$$P_{raut} = a_2(q_c - q_{cr0}), \quad (13)$$

where a_2 and q_{cr0} are calculated based on the dynamic viscosity of air, the density of water, droplet concentration, the acceleration due to gravity, the mean collection efficiency, and the critical mean droplet radius where the autoconversion begins. For cloud ice to snow,

$$P_{saut} = \max[(q_c - q_{ci0})/\Delta t, 0], \quad (14)$$

is used, where Δt is the length of time step. The critical value of autoconversion of cloud ice to snow q_{ci0} is not constant and it depends on the temperature.

The cloud amount parameterization is the same as that used in ZC and is calculated from Eq. (9). Cloud radiative properties are also calculated from cloud water content in the same manner as ZC and IS.

More complex versions of Hong's cloud schemes are also examined in the ECPC G-RSM. HONG5 employs five prognostic species including water vapor, cloud water, cloud ice, rain and snow and HONG6 employs graupel in addition to HONG5. The results using HONG3, HONG5 and HONG6 in global model simulations are very similar. However, HONG5 and HONG6 are much more expensive than HONG3 (340 % and 510 % of the SLINGO for HONG5 and HONG6, respectively), and were not used for this comparison study.

3. Data, model and experimental setup

3.1 Observational data

The International Satellite Cloud Climatology Project (ISCCP) D1 and D2 (Rossow and Schiffer 1999) data are used in this study. D1 is a 3 hourly and D2 is a monthly dataset, and both are in 280 km resolution. These datasets consist of cloud amount, cloud top pressure, cloud top temperature, cloud optical thickness and CWP, for 15 cloud types during daytime. The cloud types are defined by cloud top pressures and cloud optical thicknesses. In addition, low clouds

and middle clouds are divided into liquid and ice phase clouds (high clouds are assumed to be ice clouds). Cloud amount and CWP are used in this study. For simplicity, the 15 cloud types are combined into 3 cloud types: low, middle, and high, where low cloud is defined by cloud-top pressure $P_c > 680$ hPa, middle cloud by $440 < P_c \leq 680$ hPa, and high cloud by $P_c \leq 440$ hPa.

The relative humidity is taken from the NCEP- Department of Energy (DOE) Reanalysis 2 (R-2; Kanamitsu et al. 2002a). Maximum relative humidity in each cloud layer is used, and then interpolated to the ISCCP grid.

Monthly data from the ISCCP and R-2 for the 10-year period from 1990 to 1999 were used in this study. For the higher frequency study, 6-hourly data were also used for January and July 2000. The data in the area 60°S to 60°N is used because cloud detection errors are known to be large in the ISCCP Polar Region data (Rossow and Schiffer 1999).

For precipitation, the Global Precipitation Climatology Project (GPCP) Version 2 monthly precipitation data set (Adler et al. 2003) is used. The Earth Radiation Budget Experiment (ERBE) data set and the Surface Radiation Budget Project (SRB) data set (Stackhouse et al. 2004) are used for radiation at the top of atmosphere (TOA) and at the surface (SFC), respectively. In this study, the period of the GPCP, SRB, ISCCP and R-2 data is from 1990 to 1999 matching that of the experiment, while ERBE is from the period 1985 to 1989. We believe the comparison is considered to be still valid since it is made for long term mean.

3.2 Model

The global model version of the ECPC G-RSM is used in this study. It is based on the NCEP Seasonal Forecast Model (SFM; Kanamitsu et al. 2002b). The model horizontal resolution is T62 and 28 sigma levels in the vertical. The physics in the ECPC G-RSM include relaxed Arakawa-Schubert convection scheme (Arakawa and Schubert 1974; Moorthi and Suarez

1992) as deep convection, shallow convection, nonlocal boundary layer vertical diffusion (Hong and Pan 1996), short wave (Chou 1992) and long wave radiation parameterization (Chou et al. 1999) and Noah land surface model (Ek et al. 2003). The stratiform cloud schemes used in this study were described in Section 2.3.

High, middle, low and total cloud amounts from model simulations were calculated using maximum-random overlap assumption (Chou et al. 1998). Note that the model's cloud data may not be directly compared with the observational cloud data because the ISCCP data is a view from space, and lower clouds could be sheltered by the upper clouds (e.g. Weare 2000, 2004). For the comparison of model's three layered cloud amounts with the ISCCP, the model cloud amounts are transformed to ISCCP D2 comparable estimates following Weare (2004). The method is explained as follows: For the model high cloud, the amount should be same as that observed from space. The model mid cloud amount as observed from space, is the amount of mid cloud not sheltered by high cloud. Using the "random overlap assumption" the corrected mid cloud amount mid_asfa_cf will be expressed as;

$$mid_asfa_cf = mid_cf * (1 - high_cf). \quad (15)$$

where $high_cf$, mid_cf are the model high and mid cloud amount. Similarly, the corrected model low cloud amount low_asfa_cf is defined as;

$$low_asfa_cf = low_cf * (1 - high_cf) * (1 - mid_cf). \quad (16)$$

where low_cf is the model low cloud amount. It should be noted that these corrected cloud amounts like should only be used for comparison with ISCCP data, but not comparing the cloud amount between the models since they are affected by the clouds above. Therefore, we used both corrected and raw model cloud amounts in this paper.

CWP from model simulations were calculated using the cloud water/ice mixing ratio.

The model simulations were performed from January 1989 to December 1999 but the first year is excluded from the evaluation. The simulations are started from the R-2 analysis, and the model is integrated using daily observed sea surface temperatures (SSTs), which is interpolated from the NCEP weekly analysis (Reynolds and Smith 1994).

4. Results

4.1 Clouds

Fig.1 shows the zonally averaged total cloud amount distribution for DJF (December, January and February) and JJA (June, July and August). The output of model total cloud amount is shown in Fig.1. All simulations have their peaks of total cloud amount in low and mid-latitudes in both DJF and JJA, agreeing with observation, but with clear bias of more than 20% in most of the latitudes. Some schemes are better in some latitudes and seasons, but other schemes are better in others. Among the four schemes, IS shows somewhat better total cloud distribution than the other cloud schemes.

Zonally averaged high, middle and low cloud amount distributions for DJF are shown in Fig.2. For this verification, the corrected cloudiness as viewed from space is used to compare with the ISCCP (mid_asfa_cf, Eq. (15) and low_asfa_cf, Eq. (16)). The result for JJA was very similar and not shown. High cloud amount are better simulated in SLINGO and HONG, overestimated in IS and underestimated in ZC. For middle clouds, all simulated cloud amounts are in good agreement with the ISCCP in low latitudes, while underestimated in high latitudes. On the other hand, simulated low cloud amounts are underestimated in low latitudes, while low cloud amounts in IS and HONG are overestimated and SLINGO and ZC are underestimated. The underestimation of low cloud amounts in low latitudes and underestimation of middle cloud in high latitudes are consistent with the underestimation of simulated total cloud amounts

in extra-tropics.

Those cloud distributions are very sensitive to the empirical parameters used in each cloud scheme and adjustment of the parameter can reduce the zonal bias, although improvement of spatially varying bias is much more difficult. For example in ZC, the negative bias in high clouds is related to the small amount of cloud ice content, which is very sensitive to the critical value used for the autoconversion.

Looking at the geographical distribution of high cloud amount (Fig.3), it is clear that the pattern is fairly similar in all the cloud schemes in the tropics. Further examination showed that the high cloud amount distribution resembles that of the relative humidity distribution in all cloud schemes (not shown). This will be discussed further in Section 5. We also found that the cloud ice content affects both cloud amount distribution and simulated temperature field through cloud radiation interaction. This topic will be covered in section 4.3.

In order to compare the low level clouds among four cloud schemes, observed and simulated low cloud amounts in JJA are shown in Fig.4. Note that model raw cloud amount (low_cf , Eq. (16)) is used for comparison. Though underestimation of low cloud amounts is again seen in low latitudes, ZC, IS and HONG are apparently better than SLINGO. This minor improvement is found over subtropical ocean (Fig.4), suggesting that the cloud water scheme improves low cloud amounts due either to the simulated low level cloud water or to the interaction between the stratiform cloud and the boundary layer cloud. This improvement is also seen over land in NH mid-latitudes in JJA (Fig.4), where relative humidity is low. The 90% critical relative humidity for the formation of low cloud amount over land in SLINGO is too high during summer, resulting in negative bias. Incorporating cloud water prediction improves such cases.

Fig.5 shows zonally averaged CWP distributions for ZC, IS and HONG. CWP is mostly overestimated, except in NH mid-latitudes for ZC and HONG in DJF. This overestimation is caused by the overestimation of CWP associated with water (liquid) clouds, which are 3 to 4 times larger than observed (Fig.5d). CWP associated with ice clouds are better simulated, however, it is overestimated in IS and underestimated in ZC. HONG produced better CWP associated with ice clouds than IS and ZC in this study, which may be due to more.

4.2 Precipitation

Zonally averaged precipitation distributions for DJF and JJA (Fig.6) show that simulated precipitation is overestimated in low latitudes for all simulations. In addition, two precipitation peaks appear in the tropics, indicating double intertropical convergence zone (ITCZ). This ITCZ pattern is a common problem seen in many GCMs (e.g. Covey et al. 2003; Dai 2006). In mid and high latitudes, simulated precipitation has a good agreement with observation. From the geographical distribution of precipitation (Fig.7), IS is the best of all cloud schemes, especially in low latitude. Particularly, relative magnitude of precipitation between ITCZ and the South Pacific convergence zone (SPCZ) is closer to observation than other cloud schemes, though the amount of precipitation is still overestimated.

4.3 Temperature

Fig.8 shows the zonally averaged vertical cross section of the temperature difference between R-2 and each cloud scheme in DJF. In general, cold biases exist in the stratosphere in all experiments, which is not sensitive to cloud schemes. In the troposphere, all simulations show fairly small temperature error compared to R-2, especially in low latitudes, where the temperature difference is under 2 °C. However, in extra-tropics, a warm bias appears in the upper troposphere, especially in ZC and IS near tropopause in the summer hemisphere, which

seems to be related to small cloud ice content and associated cloud radiative properties. In our sensitivity test, the warm bias is much worse in the simulation when the default autoconversion critical temperature quoted in the original paper (Zhao and Carr 1997) is used. In the current simulation, smaller critical value is used to reduce the warm bias. The amount of cloud water and ice may not be the only cause of the warm bias, since the warm bias does not appear in HONG, in which the amount of CWP is similar to IS in the summer hemisphere (Fig. 5).

4.4 Radiation

Fig.9 shows the comparison of observed and simulated upward longwave and shortwave radiation fluxes (LWu, SWu) at the top of the atmosphere (TOA), and downward longwave and shortwave radiation (LWd, SWd) at the surface (SFC) for DJF. The LWu at the TOA (Fig.9a) from IS has the smallest bias from ERBE, especially in mid-latitudes. Those biases are strongly related to high cloud distributions (Fig.2a). However, since high cloud amount in IS is overestimated, we think that the underestimation of long wave emissivity from CWP, or the underestimation of CWP itself in the model, is compensating the overestimation of cloud amount. In addition, the cloud top height and temperature also affects simulated TOA LWu. In this context, improvement of clouds associated with convection and associated CWP seems to be needed.

SFC LWd (Fig.9c) shows an opposite bias to that of TOA LWu. All cloud schemes show common negative bias of about 20 W m^{-2} in low latitudes, while the error is different for each cloud scheme in mid-latitudes. Those biases in the simulations are strongly related to low cloud distributions (Fig.2c). It is clear that changing stratiform cloud schemes does not significantly improve the underestimation of SFC LWd in low latitudes.

In the tropics, TOA SWu is overestimated in IS, while it is underestimated in the others.

In all the cloud schemes, the area of large SWu bias roughly matches the area of large convective precipitation, suggesting that the stronger sensitivity of convective cloudiness to precipitation rate is needed to reduce the bias. In mid-latitude, it is clear that all the cloud schemes except SLINGO simulate TOA SWd well. We also observe that SFC SWd is improved in those cloud schemes. This is considered to be due to the explicit prediction of cloud water in those cloud schemes, which allows more physical estimation of the cloud radiation property. Note that the SLINGO does not predict cloud water and the cloud radiation property is simply assumed as a function of temperature. Looking at the detail, although the ZC TOA SWu agrees with observation in most of the latitudes, it has a large error, around 60S, similar to SLINGO. This is considered to be due to less high and middle cloud amount (Fig. 3).

4.5 Differences of formulations

In this section, we try to interpret the differences presented above from the difference in the formulation of cloud water and cloudiness prediction. Particularly, we will focus on the treatment of cloud ice. The autoconversion of cloud ice to snow and the falling ice are the two processes that affected the mean cloud ice fields. In ZC and IS, autoconversion of cloud ice to snow is formulated as Eq. 8, but the effect of falling ice is not considered. On the other hand, HONG considered both the autoconversion and the falling ice. As shown in Fig.5c, HONG predicted better ice CWP distribution than ZC and IS, though it is underestimated compared to the ISCCP. However, it is inconsistent that ZC produced lower cloud water (ice) content, though ZC didn't consider the falling ice. As shown in Eq. 8, the threshold value of cloud ice to snow is smaller than that in the original paper. This mimics the effect of falling ice and, as a result, the cloud ice distribution does not suffer from overestimation. It should be noted that the parameter value used in Eq. 8 is unrealistically low, which caused the underestimation of ice CWP

compared to ISCCP (Fig.5c).

In IS, both cloud ice and high cloud amount were overestimated. This may be due to the fact that IS did not consider the falling ice. In addition, from the cloud amount prognostic Eq. 11, the cloud amount does not change when precipitation occurs in IS, while it decreases in ZC and HONG since cloud water/ice decreases when precipitation occurs. It is necessary to perform observational work to study the relation between precipitation and change in cloudiness.

4.6 Summary of the comparison of cloud schemes

In summary, four stratiform cloud schemes show underestimation of total cloud amount. The distribution of high, middle and low cloud amounts for each cloud scheme are somewhat similar to observation but with many problems. The distribution is very sensitive to parameters in the cloud scheme. There is some indication that the prediction of cloud water improves the simulation, particularly over dry areas, but the improvement is minor. The stratiform cloud scheme affects convective precipitation distribution. However, simulated precipitation is overestimated with a double ITCZ problem in most of the schemes. All the simulations suffer from systematic temperature error, which is also sensitive to the parameters in the cloud scheme, particularly to the auto conversion critical temperature. The TOA and SFC radiation flux shows no cloud scheme stands out in all aspects, but some advantage is found for schemes in which predicted cloud water interacts with radiation. Simulated SW radiation fluxes are improved when a cloud water scheme is used, however, biases in LW radiation fluxes are still large in many of the schemes.

Although, the IS scheme outperforms the other schemes in some respects, its advantage is small. Thus, we are forced to conclude that no one cloud scheme is better than others in all respects. The simulation is very sensitive to parameters in the cloud schemes. Without adjusting

the parameter for each scheme for optimal performance, it is very difficult to arrive at any clear conclusions regarding which scheme to choose. Even if such an effort is possible, the cloud scheme may behave differently in different modeling systems. This is somewhat in contrast to other parameterization schemes, such as convection, which are parameter dependent, but much less sensitive than cloud parameterization.

5. Relationships between relative humidity, cloud amount and cloud water

From the results obtained above, it becomes clear that the pattern of simulated cloud amount is strongly controlled by the relative humidity in mid and high latitudes where stratiform clouds are dominant, especially for high clouds. Of course this is true for SLINGO, but it is also true for the schemes with cloud water prediction, for which cloud amount is a function of cloud water and relative humidity (except the IS scheme), but the cloudiness is formulated in such a way that it depends more strongly on relative humidity. In reality, Eq. 9 is formulated to increase cloud amount as relative humidity increases when cloud water is constant and to increase the dependency of cloudiness to relative humidity when cloud water content is small (Randall 1995; Xu and Randall 1996).

Some statistical relations between relative humidity and cloud amount have been investigated e.g., Saito and Baba (1988). Those relations have been used for cloud parameterizations (Teixeira 2001). The relationship between cloud amount, relative humidity and cloud water was first proposed by Randall (1995). Their scheme is based on a cloud resolving model simulation. The cloudiness is computed as a function of simulated spatially averaged relative humidity and cloud water, by assuming cloud formation when the cloud water size exceeds a predetermined size. We have decided to re-examine this relationship based on

ISCCP data, which is a large-scale observation, potentially more valid for coarse resolution model parameterization. For this purpose, we generated several scatter diagrams of the relation between cloud amount, cloud water content and relative humidity for high, middle and low clouds from model simulations and from the combination of ISCCP observation and NCEP-DOE Reanalysis. For cloud observation, the three layered cloud amount and cloud water from ISCCP are used. For simulations, CWP at each cloud layer was calculated from the output of cloud water content at pressure levels. Maximum relative humidity in each cloud layer is used for the relative humidity corresponding to low, middle and high clouds, and then interpolated to the ISCCP grid for both the NCEP-DOE Reanalysis and the simulations. The range of pressure levels for high, middle and low clouds were taken from ISCCP definition. These pressure layers roughly correspond to the cloud layers in the ECPC G-RSM. Scatter diagrams of cloud water vs. cloud amount and relative humidity vs. cloud amount were made using monthly mean data. To limit our attention to stratiform clouds, we restricted the domain to 30°N to 60°N. Similar computations were made in SH mid-latitude and the results were very similar.

Fig.10 shows the scatter diagrams of cloud amount against relative humidity and cloud amount against cloud water for high cloud in model simulations, SLINGO, ZC, IS and HONG. SLINGO has only one plot in Fig.10 because cloud water is not predicted. It is shown that all model simulations have positive correlations between relative humidity and cloud amount. The sensitivity (slope of the line) of cloud amount to relative humidity is different for each simulation. IS shows the highest sensitivity of RH to cloudiness among the four simulations, and HONG and SLINGP have about the same sensitivities. ZC has lower sensitivity than others. The lower sensitivity of ZC compared to HONG can be explained by the smaller cloud ice in ZC. The range of relative humidity and cloud amount is different for different cloud schemes.

Sensitivities of cloud amount against cloud water are also different from each other. The range of CWP in ZC is small and the range of cloud amount for a given cloud water is large, about 40 %. In IS, the range of CWP is larger and the sensitivity of cloud amount to a given cloud water is smaller compared to ZC. HONG shows higher sensitivity than IS. This difference of sensitivities seems to be caused by the different methods of calculating cloud amount. Most likely, those sensitivities can be changed by using different parameters in the cloud schemes.

The corresponding scatter diagram from ISCCP observation is shown in Fig.11. In making these figures, cloud amount and CWP for high thick cloud was not used because most of the high thick cloud is categorized as a deep convection (Rossow and Schiffer 1999). It is clear that the range of cloud amount against a given relative humidity is larger in observation than in simulations. Positive correlations are seen for middle and low clouds, but the range of cloud amount against relative humidity is larger than in simulations. In contrast, there is a strong positive correlation between cloud water and cloud amount, i.e., the range of cloud amount against given cloud water is narrower than those seen in the relationships between relative humidity and cloud amount.

From the results shown above, it seems that there may be an advantage to formulating cloud amount from cloud water rather than diagnosing cloud amount from relative humidity, or from the combination of relative humidity and cloud water. Apparently, the scatter diagrams showed that in the current cloud schemes, cloud amount is too dependent on relative humidity, while in reality it should depend more strongly on cloud water. An additional merit of using only cloud water for the cloud amount is that cloudiness associated with convection and boundary layer cloud, currently parameterized independently from stratiform cloud, could perhaps be combined into one simple formulation.

As a preliminary study, we proposed a formula for cloud amount based solely on cloud water content, by removing the dependency to relative humidity from Randall's (1995) formulation:

$$C = 1 - \exp(-\beta q_c), \quad (17)$$

where q_c is mean cloud water content and β is a constant to be determined from observational data. β can be a function of height (and also of season and latitude). To determine the constant β , ISCCP 6-hourly D1 data and R-2 data are used. The values obtained from January 2000 are 1.6×10^5 , 0.8×10^5 , and 1.2×10^5 , for high, middle and low clouds, respectively. When βq_c is small, cloud amount derived from Eq. 17 can be approximated by $C = \beta q_c$. It implies the in-cloud water content q_{ci} , which is defined as q_c divided by C , is constant ($=\beta^{-1}$). On the other hand, when βq_c is not small, q_{ci} is not constant.

Fig.12 shows the zonal and monthly mean observed cloud amount and diagnosed cloud amount from three methods; 1) relative humidity only, based on Slingo's formula, 2) both relative humidity and cloud water based on Randall's formula, and 3) only cloud water based on the new formula in this study using ISCCP cloud water data during July 2000 (independent data from the ones the coefficient β is computed). It is clear that obtained cloud amount is much better when the proposed parameterization is used.

Unfortunately, the direct application of this formulation to model simulation is found to be not so straightforward. The simulation was found to be much worse than the ones with original formulation. Of particular concern is the numerical model's skill to simulate the cloud water distribution correctly without significant bias. In addition, noisiness in cloud water such as due to the Gibbs phenomenon in spectral model, has been found to cause undesirable results. Although some of these problems can be overcome by introducing some sort of bias correction

and critical minimum cloud water for the cloud formation, we found that it is necessary to further improve the simulation of the spatial distribution of cloud water for the new scheme to produce improved simulation.

It needs to be mentioned here that in this study, relative humidity from the reanalysis (R-2) is used to estimate the relation between cloud amount and relative humidity. The R-2 (and NCEP/NCAR Reanalysis) does not distinguish the saturation vapor pressure over water and ice (always use over water), which introduces significant error in the value of relative humidity at low temperatures. Since observations of relative humidity at upper troposphere (and stratosphere) are not abundant and difficult to verify the reanalysis, arguing the relation between relative humidity and cloudiness at low temperature may be problematic. Recently, Gettleman et al. (2006b) presented that relative humidity at low temperature can be obtained from satellite observations. Gettleman et al. (2006a) examined supersaturated regions in the upper troposphere and showed that it is very frequent in the extratropical upper troposphere. These studies may be useful to further examine the relative humidity-cloudiness relationships. Some physically based parameterization for ice clouds are recently suggested by Kärcher et al. 2006, however, our knowledge of ice cloud in upper troposphere is far from satisfactory and its parameterization requires further efforts.

6. Conclusions

In this study, four stratiform cloud parameterizations are compared by examining the seasonal mean fields forced by the observed SST using the ECPC G-RSM. Since our focus is stratiform cloud, all other physical processes are fixed, including convective cloud and boundary layer topped cloud. Simulated fields are compared to observation and reanalysis data, including

ISCCP for clouds, GPCP for precipitation, ERBE and SRB for radiation and R-2 for temperature.

The following four cloud schemes are examined: 1) Slingo scheme (SLINGO), in which cloud amount is diagnosed only from relative humidity. 2) Zhao and Carr scheme (ZC), which has the cloud water/ice mixing ratio as a predictive variable, and cloud amount is diagnosed from relative humidity and the cloud water/ice mixing ratio based on Randall's (1995) formula. 3) Iacobellis and Somerville scheme (IS), which predicts both the cloud water/ice mixing ratio and cloud amount. 4) Hong scheme (HONG), in which the rain/snow mixing ratio in addition to the cloud water/ice mixing ratio are predicted, and cloud amount is diagnosed from relative humidity and the cloud water/ice mixing ratio based on Randall's formula.

No stratiform cloud parameterization performed better than others in all respects in simulating observed cloudiness, radiation and the atmospheric temperature structure. This result may be strongly influenced by the fact that the key parameters in the stratiform cloud schemes were primarily taken from the original papers and no special adjustment was performed to improve the simulation for each stratiform cloud scheme for the model used in this study (except for some schemes which resulted in very large systematic error). Furthermore, our limited experiments showed that the simulation is very sensitive to the parameters such as the critical temperature for autoconversion from cloud water to ice. In this regard, it may not be appropriate to evaluate the stratiform cloud schemes against observations without carefully adjusting the parameters for each scheme. Moreover, since parameter adjustment itself is quite empirical and unphysical in some respect, a physically meaningful comparison of the schemes becomes very difficult. In a word, it is very difficult to choose one particular stratiform cloud scheme from a comparison of simulated cloud with observation, since every scheme can be *tuned* to perform better. This is somewhat in contrast to convective parameterization, which has tunable

parameters but the performance is less sensitive to the change in parameters.

Considering these limitations, we decided to look at the results that have more general implications, which are summarized as follows:

1. The simulated cloudiness is more or less the same for all the schemes. Only the IS scheme, which predicts cloudiness, seems to distinguish itself from others, but the improvement is not very large.
2. The simulated cloud water distribution is also more or less the same for ZC, IS and HONG. The inclusion of more complex cloud physics does not significantly change the cloud water distribution.
3. Incorporation of cloud water simulates more clouds in dry areas, indicating that those schemes may have more general applications.
4. There is a strong interaction between parameterized stratiform clouds, boundary layer clouds and convective clouds. In many occasions, the boundary layer cloud dominates the total cloud cover, which is important for atmosphere and ocean coupled modeling.
5. There is a strong interaction between parameterized cloud and convective precipitation.
6. Incorporation of the radiative property of cloud water and ice has a strong impact on the simulated temperature bias and radiation fields.

Comparing further with observed ISCCP cloudiness and cloud water and NCEP/DOE Reanalysis-2 relative humidity, we found the following:

1. In all schemes examined in this study, the cloud amount is controlled mostly by relative humidity. The influence of cloud water is secondary.
2. In the observation, the cloudiness is more strongly controlled by cloud water than by relative

humidity.

A new formula of cloudiness based only on cloud water was proposed and tested using independent observed cloud water. The formula provides a better match with observed cloudiness than relative humidity based schemes or relative humidity and cloud water based schemes. However, the application of this new scheme is still limited since it directly reflects the error and bias of the simulated cloud water, which seems to be significant and more difficult to simulate correctly than the relative humidity.

Considering that the convective and boundary layer clouds are also dominant in the simulations, it is desirable to develop a cloud scheme which encompasses all these types of clouds. As mentioned before, variety of parameterizations exists because the cloud parameterization problem is very difficult, but in principle, one (or something more unified) parameterization should exist in the future. The cloudiness parameterization based only on cloud water may be a step towards a unified cloudiness parameterization.

Acknowledgements

We thank Drs. John Roads and Ming Ji for their support throughout the study. This study was supported by NSC 95-211-M133 -001 -AP4 and NOAA NA17RJ1231. The views expressed herein are those of the authors and do not necessarily reflect the views of NOAA. We thank Ms. Diane Boomer for improving the readability of the paper. The ISCCP, ERBE and SRB data sets were obtained from the NASA Langley Research Center Atmospheric Science Data Center.

REFERENCES

- Adler, R. F., and Coauthors, 2003: The version-2 Global Precipitation Climatology Project (GPCP) monthly precipitation analysis (1979-present), *J. Hydromet.*, **4**, 1147-1167.
- Arakawa, A., and W. H. Schubert, 1974: Interaction of a cumulus cloud ensemble with the large-scale environment, Part I. *J. Atmos. Sci.*, **31**, 674-701.
- Bony, S., and K. A. Emanuel, 2001: A parameterization of the cloudiness associated with cumulus convection; evaluation using TOGA COARE data. *J. Atmos. Sci.*, **58**, 3158-3183.
- Boville, B. A., P. J. Rasch, J. J. Hack, and J. R. McCaa, 2006: Representation of clouds and precipitation processes in the Community Atmosphere Model version 3 (CAM3). *J. Climate*, **19**, 2184-2198.
- Bower, K. N., T. W. Choullarton, J. Latham, J. Nelson, M. B. Baker, and J. Jenson, 1994: A parameterization of warm clouds for use in atmospheric general circulation models. *J. Atmos. Sci.*, **51**, 2722-2732.
- Bretherton, C. S., J. R. McCaa, and H. Grenier, 2004a: A new parameterization for shallow cumulus convection and its application to marine subtropical cloud-topped boundary layers. Part I: Description and 1D results. *Mon. Wea. Rev.*, **132**, 864-882.
- Bretherton, C. S., T. Uttal, C. W. Fairall, S. E. Yuter, R. A. Weller, D. Baumgardner, K. Comstock, R. Wood, and G. B. Raga, 2004b: The EPIC 2001 stratocumulus study. *Bull. Amer. Meteor. Soc.*, **85**, 967-977.
- Chou, M. -D., 1992: A solar radiation model for use in climate studies. *J. Atmos. Sci.*, **49**, 762-772.
- Chou, M. -D., K. -T. Lee, S. -C. Tsay, and Q. Fu, 1999: Parameterization for cloud longwave scattering for use in atmospheric models. *J. Climate*, **12**, 159-169.

- Chou, M. -D., M. J. Suarez, C. -H. Ho, M. M. -H. Yan, and K. -T. Lee, 1998: Parameterizations for cloud overlapping and shortwave single-scattering properties for use in general circulation and cloud ensemble models. *J. Climate*, **11**, 202-214.
- Collins, W. D., and Coauthors, 2006: The formulation and atmospheric simulation of the Community Atmosphere Model version 3 (CAM3). *J. Climate*, **19**, 2144-2161.
- Covey, C., K. M. AchutaRao, U. Cubasch, P. Jones, S. J. Lambert, M. E. Mann, T. J. Phillips, and K. E. Taylor, 2003: An overview of results from the Coupled Model Intercomparison Project. *Global Planet. Change*, **37**, 103-133.
- Dai, A., 2006: Precipitation characteristics in eighteen coupled climate models. *J. Climate*, **19**, 4605-4630.
- Delworth, T. L., and Coauthors, 2006: GFDL's CM2 global coupled climate models. Part I: formulation and simulation characteristics. *J. Climate*, **19**, 643-674.
- Dudhia, J., 1989: Numerical study of convection observed during the winter monsoon experiment using a mesoscale two-dimensional model. *J. Atmos. Sci.*, **46**, 3077-3107.
- Duynderke, P. G., and J. Teixeira, 2001: Comparison of the ECMWF reanalysis with FIRE I observations: Diurnal variation of marine stratocumulus. *J. Climate*, **14**, 1466-1478.
- Ebert, E. E., and J. A. Curry, 1992: A parameterization of ice cloud optical properties for climate models. *J. Geophys. Res.*, **97**, 3831-3836.
- Ek, M. B., K. E. Mitchell, Y. Lin, E. Rogers, P. Grunmann, V. Koren, G. Gayno, and J. D. Tarpley, 2003: Implementation of Noah land surface model advances in the National Centers for Environmental Prediction operational mesoscale Eta model. *J. Geophys. Res.*, **108** (D22), 8851, doi:10.1029/2002JD003296.
- Fowler, L. D., D. A. Randall, and S. A. Rutledge, 1996: Liquid and ice cloud microphysics in the

- CSU general circulation model. Part I: Model description and simulated microphysical processes. *J. Climate*, **9**, 489-529.
- The GFDL Global Atmospheric Model Development Team, 2004: The new GFDL global atmosphere and land model AM2-LM2: Evaluation with prescribed SST simulations. *J. Climate*, **17**, 4641-4673.
- Gettelman, A., E. J. Fetzer, A. Eldering, F. W. Irion, 2006a: The global distribution of supersaturation in the upper troposphere from the atmospheric infrared sounder. *J. Climate*, **19**, 6089-6103.
- Gettelman, A., W. D. Collins, E. J. Fetzer, A. Eldering, F. W. Irion, P. B. Duffy, and G. Bala, 2006b: Climatology of upper-tropospheric relative humidity from the atmospheric infrared sounder and implications for climate. *J. Climate*, **19**, 6104-6121.
- Gordon, C., C. Cooper, C. A. Senior, H. Banks, J. M. Gregory, T. C. Johns, J. F. B. Mitchell, and R. A. Wood, 2000: The simulation of SST, sea ice extents and ocean heat transports in a version of the Hadley Centre coupled model without flux adjustments. *Clim. Dyn.*, **16**, 147-168.
- Hong, S. -Y., J. Dudhia, and S. -H. Chen, 2004: A revised approach to ice microphysical processes for the bulk parameterization of clouds and precipitation. *Mon. Wea. Rev.*, **132**, 103-120.
- Hong, S. -Y., H. -M. H. Juang, and Q. Zhao, 1998: Implementation of prognostic cloud scheme for a regional spectral model. *Mon. Wea. Rev.*, **126**, 2621-2639.
- Hong, S. -Y., and H. -L. Pan, 1996: Nonlocal boundary layer vertical diffusion in a medium-range forecast model. *Mon. Wea. Rev.*, **124**, 2322-2339.
- Iacobellis, S. F., and R. C. J. Somerville, 2000: Implications of microphysics for cloud-radiation

- parameterizations: Lessons from TOGA COARE. *J. Atmos. Sci.*, **57**, 161-183.
- Kanamitsu, M., W. Ebisuzaki, J. Woollen, S. -K. Yang, J. J. Hnilo, M. Fiorino, and G. L. Potter, 2002a: NCEP-DOE AMIP-II Reanalysis (R-2). *Bull. Amer. Meteor. Soc.*, **83**, 1631-1643.
- Kanamitsu, M., and Coauthors, 2002b: NCEP dynamical seasonal forecast system 2000. *Bull. Amer. Meteor. Soc.*, **83**, 1019-1037.
- Kärcher, B., J. Hendricks, and U. Lohmann, 2006: Physically based parameterization of cirrus cloud formation for use in global atmospheric models. *J. Geophys. Res.*, **111**, D01205, doi:10.1029/2005JD006219.
- Lin, Y. -L., R. D. Farley, and H. D. Orville, 1983: Bulk parameterization of the snow field in a cloud model. *J. Appl. Meteor.*, **22**, 1065-1092.
- Lohmann, U., N. McFarlane, L. Levkov, K. Abdella, and F. Albers, 1999: Comparing different cloud schemes of a single column model by using mesoscale forcing and nudging technique. *J. Climate*, **12**, 438-461.
- Moorthi, S., and M. J. Suarez, 1992: Relaxed Arakawa-Schubert: A parameterization of moist convection for general circulation models. *Mon. Wea. Rev.*, **120**, 978-1002.
- Randall, D. A., 1995: Parameterizing fractional cloudiness produced by cumulus detrainment. Workshop on cloud microphysics parameterizations in global atmospheric circulation models, Kananaskis, Alberta, Canada, 23-25 May 1995, WCRP-90, WMO/TD-No.713, 1-16.
- Reynolds, R. W., and T. M. Smith, 1994: Improved global sea surface temperature analyses using optimum interpolation. *J. Climate*, **7**, 929-948.
- Rossow, W. B., and R. A. Schiffer, 1999: Advances in understanding clouds from ISCCP. *Bull. Amer. Meteor. Soc.*, **80**, 2261-2287.

- Rotstayn, L. D., B. F. Ryan, and J. J. Katzfey, 2000: A scheme for calculation of the liquid fraction in mixed-phase stratiform clouds in large-scale models. *Mon. Wea. Rev.*, **128**, 1070-1088.
- Rutledge, S. A., and P. V. Hobbs, 1983: The mesoscale and microscale structure and organization of clouds and precipitation in midlatitude cyclones. VIII: A model for the “seeder-feeder” process in warm-frontal rainbands. *J. Atmos. Sci.*, **40**, 1185-1206.
- Saito, K., and A. Baba, 1988: A statistical relation between relative humidity and the GMS observed cloud amount. *J. Meteor. Soc. Japan*, **66**, 187-192.
- Senior, C. A., and J. F. B. Mitchell, 1993: Carbon dioxide and climate: The impact of cloud parameterization. *J. Climate*, **6**, 393-418.
- Slingo, J. M., 1987: The development and verification of a cloud prediction scheme for the ECMWF model. *Quart. J. Roy. Meteor. Soc.*, **113**, 899-927.
- Slingo, A., 1989: A GCM parameterization for the shortwave radiation properties of water clouds. *J. Atmos. Sci.*, **46**, 1419-1427.
- Slingo, A., and J. M. Slingo, 1991: Response of the National Center for Atmospheric Research Community Climate Model to improvements in the representation of clouds. *J. Geophys. Res.*, **96**, 15,341-15,357.
- Smith, R. N. B., 1990: A scheme for predicting layer clouds and their water content in a general circulation model. *Quart. J. Roy. Meteor. Soc.*, **116**, 435-460.
- Sommeria, G., and J. W. Deardorff, 1977: Subgrid-scale condensation in models of nonprecipitation clouds. *J. Atmos. Sci.*, **34**, 344-355.
- Stackhouse, P. W., Jr., and Coauthors, 2004: 12-year Surface Radiation Budget data set. *GEWEX News*, **14**, 10-12.

- Sundqvist, H., 1978: A parameterization scheme for non-convective condensation including prediction of cloud water content. *Quart. J. Roy. Meteor. Soc.*, **104**, 677-690.
- Sundqvist, H., E. Berge, and J. E. Kristjánsson, 1989: Condensation and cloud parameterization studies with a mesoscale numerical weather prediction model. *Mon. Wea. Rev.*, **117**, 1641-1657.
- Stevens, B. and Coauthors, 2001: Simulations of trade wind cumuli under a strong inversion. *J. Atmos. Sci.*, **58**, 1870-1891.
- Stevens, B. and Coauthors, 2005: Evaluation of large-eddy simulations via observations of nocturnal marine stratocumulus. *Mon. Wea. Rev.*, **133**, 1443-1462.
- Teixeira, J., 2001: Cloud fraction and relative humidity in a prognostic cloud fraction scheme. *Mon. Wea. Rev.*, **129**, 1750-1753.
- Teixeira, J. and T. F. Hogan, 2002: Boundary layer clouds in a global atmospheric model: Simple cloud cover parameterizations. *J. Climate*, **15**, 1261-1276.
- Tiedtke, M., 1993: Representation of clouds in large-scale models. *Mon. Wea. Rev.*, **121**, 3040-3061.
- Tompkins, A. M., 2002: A prognostic parameterization for the subgrid-scale variability of water vapor and clouds in large-scale models and its use to diagnose cloud cover. *J. Atmos. Sci.*, **59**, 1917-1942.
- Weare, B. C., 2000: Near-global observations of low clouds. *J. Climate*, **13**, 1255-1268.
- Weare, B. C., 2004: A comparison of AMIP II model cloud layer properties with ISCCP D2 estimates. *Clim. Dyn.*, **22**, 281-291.
- Wyser, K., 1998: The effective radius in ice clouds. *J. Climate*, **11**, 1793-1802.
- Xu, K. -M., and D. A. Randall, 1996: A semiempirical cloudiness parameterization for use in

climate models. *J. Atmos. Sci.*, **53**, 3084-3102.

Zhao, Q., and F. H. Carr, 1997: A prognostic cloud scheme for operational NWP models. *Mon. Wea. Rev.*, **125**, 1931-1953.

Figure captions:

Fig.1 Zonally averaged distribution of observed and simulated total cloud amount (%) in (a) DJF and (b) JJA for 1990 – 1999. ISCCP (thick solid line), SLINGO (thin solid line), ZC (dashed line), IS (dotted line) and HONG (dot-dashed line) are shown.

Fig.2 As in Fig.1, but for (a) high, (b) middle and (c) low cloud amount in DJF.

Fig.3 Geographical distributions of observed and simulated high cloud amount (%) in DJF for 1990 – 1999. (a) ISCCP, (b) SLINGO, (c) ZC, (d) IS and (e) HONG are shown. Contour interval is 10 %. Light stippled area is for 10~30 and heavy stippled for above 30 %.

Fig.4 As in Fig.3, but for high cloud amount (%) in DJF. Contour interval is 10 %. Light stippled area is for 30~50 and heavy stippled for above 50 %.

Fig.5 As in Fig.1, but for cloud water path (g m^{-2}) in (a) DJF, (b) JJA, DJF for (c) ice clouds and (d) water (liquid) clouds. ISCCP (thick solid line), ZC (dashed line), IS (dotted line) and HONG (dot-dashed line) are shown.

Fig.6 As in Fig.1, but for precipitation (mm day^{-1}). Observation is from GPCP.

Fig.7 As in Fig.3, but for precipitation (mm day^{-1}) in DJF. (a) GPCP observed, (b) SLINGO, (c) ZC, (d) IS and (e) HONG are displayed. Contour interval is 3 mm day^{-1} . Light stippled area

is for between 3 and 9 and heavy stippled for above 9 mm day⁻¹.

Fig.8 Zonally averaged temperature differences (°K) from R-2 for (a) SLINGO, (b) ZC, (c) IS and (d) HONG in DJF for 1990 – 1999. Contour indicates ± 1 °K and then every 2 °K. Area of light stippling is for below -2 and heavy stippling is for above 2.

Fig.9 Differences of zonally averaged radiation fluxes between simulation and observation in DJF. (a) upward longwave radiation flux at TOA, (b) upward shortwave radiation flux at TOA, (c) downward longwave radiation flux at SFC and (d) downward shortwave radiation flux at SFC. Observed radiation fluxes are from ERBE for TOA and SRB for SFC. The period of observation is 1990-1999 for SRB and 1985-1989 for ERBE. Unit is in W m⁻².

Fig. 10 Scatter diagrams of relative humidity vs. cloud amount (left panels) and cloud water path vs. cloud amount (right panels) for high cloud from SLINGO (a), ZC (b and c), IS (d and e) and HONG (f and g) simulations over the area [0-360, 30°N-60°N] during January 1999 – December 1999. Units of relative humidity and cloud amount are in percent and cloud water path in g m⁻².

Fig. 11 Scatter diagrams of relative humidity vs. cloud amount (left panels) and cloud water path vs. cloud amount (right panels) for high (a and b), middle (c and d) and low clouds (g and h) from observation (ISCCP) and reanalysis (R-2) over the area [0-360, 30°N-60°N] during January 1999 – December 1999. Units of relative humidity and cloud amount are in percent and cloud water path in g m⁻².

Fig. 12 Monthly averaged zonal mean cloud amount (%) from ISCCP (cross marks), cloud amount calculated from relative humidity only based on Slingo (1987) (dotted line), calculated from relative humidity and cloud water based on Randall (1995) (dashed line) and calculated from cloud water only based on new formula (solid line). (a) High, (b) middle and (c) low clouds for July 2000 are shown. For the calculation, 6 hourly cloud water from ISCCP D1 data and relative humidity from R-2 were used.

Table.1 Summary of cloud parameterizations.

Code	Number of cloud water prognostic variables	Cloud water prognostic variables	Stratiform cloud	Convective cloud	Boundary layer cloud	Efficiency (SLINGO =100%)
SLINGO	0	(none)	diagnosed from RH (Slingo 1987)	diagnosed from convective precipitation (Slingo 1987)	diagnosed from inversion strength and RH (Slingo 1987)	100%
ZC	1	qc/qi	diagnosed from RH and qc/qi (Randall 1995)	same as SLINGO	same as SLINGO	110%
IS	1	qc/qi	predicted (Tiedtke 1993)		same as SLINGO	150%
HONG	2	qc/qi qr/qs	same as ZC	same as SLINGO	same as SLINGO	240%

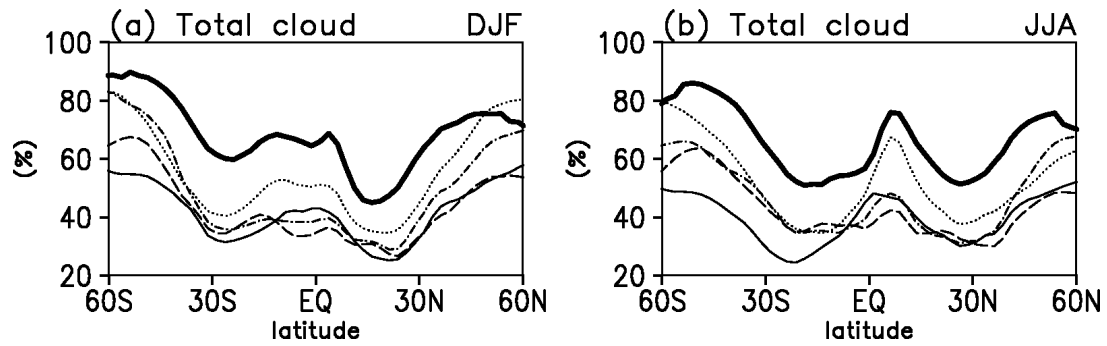


Fig.1 Zonally averaged distribution of observed and simulated total cloud amount (%) in (a) DJF and (b) JJA for 1990 – 1999. ISCCP (thick solid line), SLINGO (thin solid line), ZC (dashed line), IS (dotted line) and HONG (dot-dashed line) are shown.

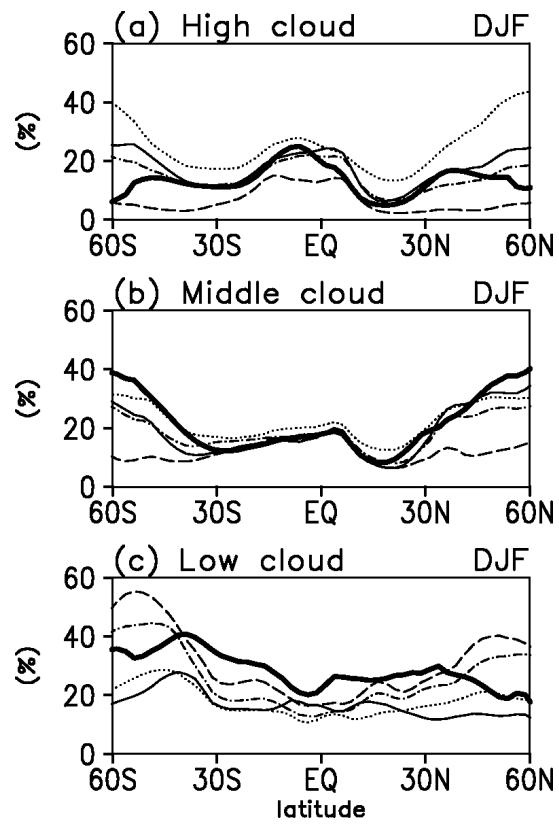


Fig.2 As in Fig.1, but for (a) high, (b) middle and (c) low cloud amount in DJF.

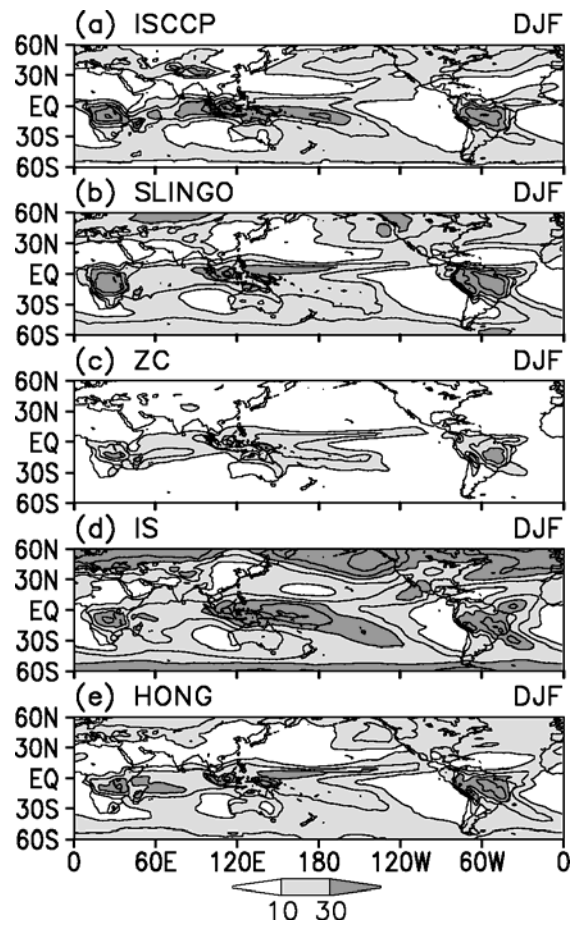


Fig.3 Geographical distributions of observed and simulated high cloud amount (%) in DJF for 1990 – 1999. (a) ISCCP, (b) SLINGO, (c) ZC, (d) IS and (e) HONG are shown. Contour interval is 10 %. Light stippled area is for 10~30 and heavy stippled for above 30 %.

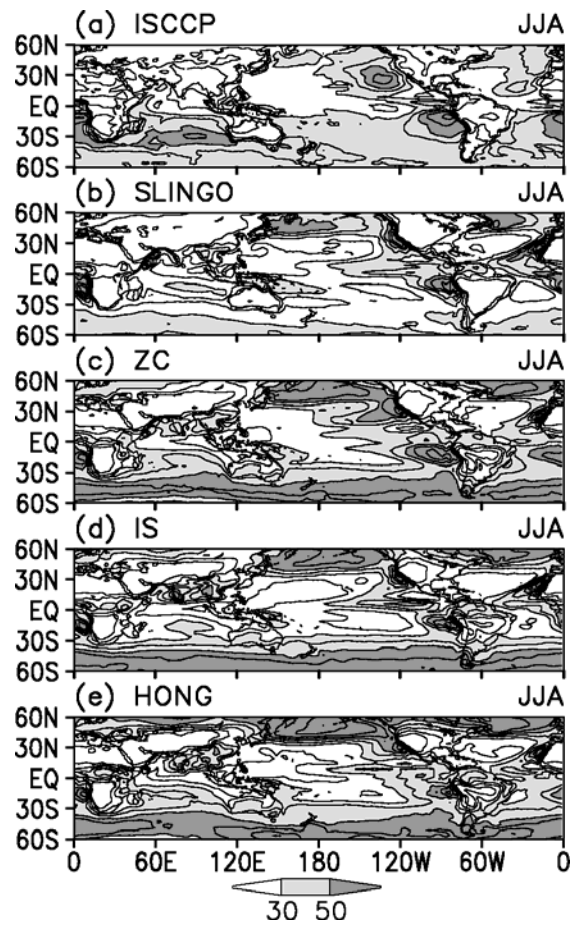


Fig.4 As in Fig.3, but for low cloud amount (%) in JJA. Contour interval is 10 %. Light stippled area for 30~50 and heavy stippled for above 50 %.

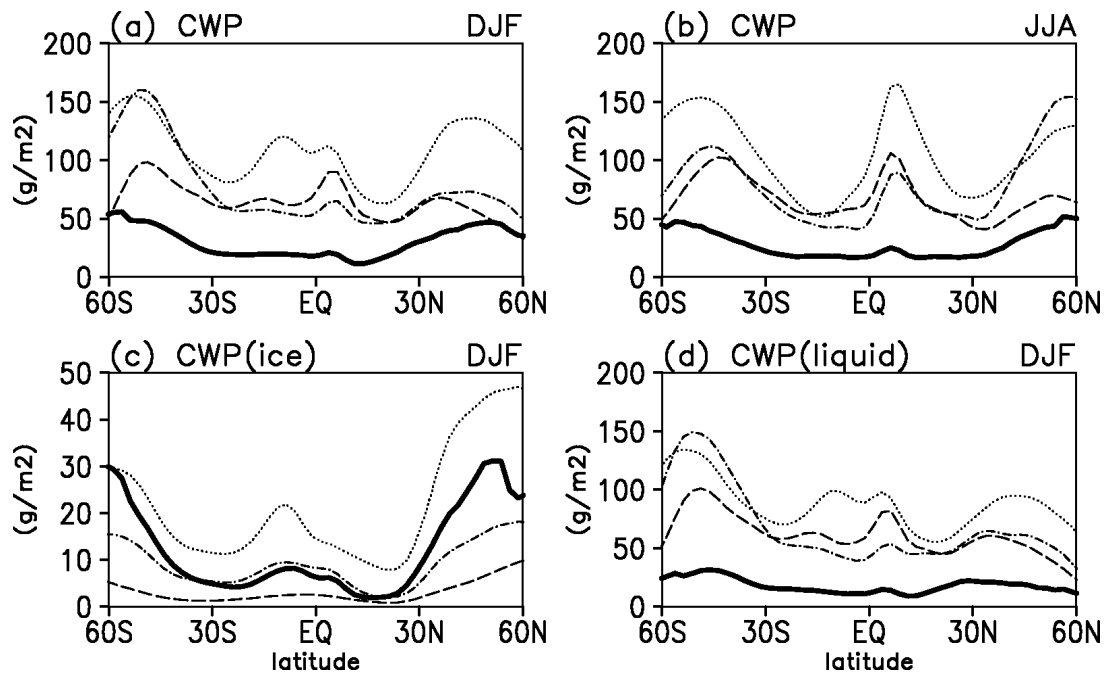


Fig.5 As in Fig.1, but for cloud water path (g m^{-2}) in (a) DJF, (b) JJA, DJF for (c) ice clouds and (d) water (liquid) clouds. ISCCP (thick solid line), ZC (dashed line), IS (dotted line) and HONG (dot-dashed line) are shown.

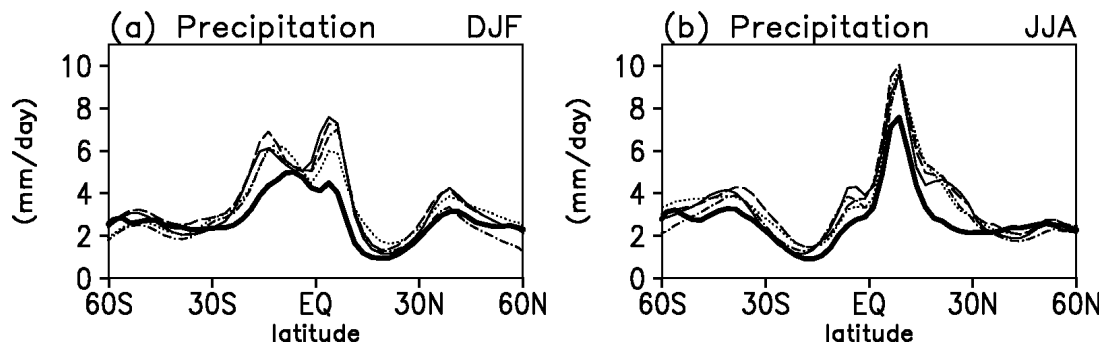


Fig.6 As in Fig.1, but for precipitation (mm day^{-1}). Observation is from GPCP.

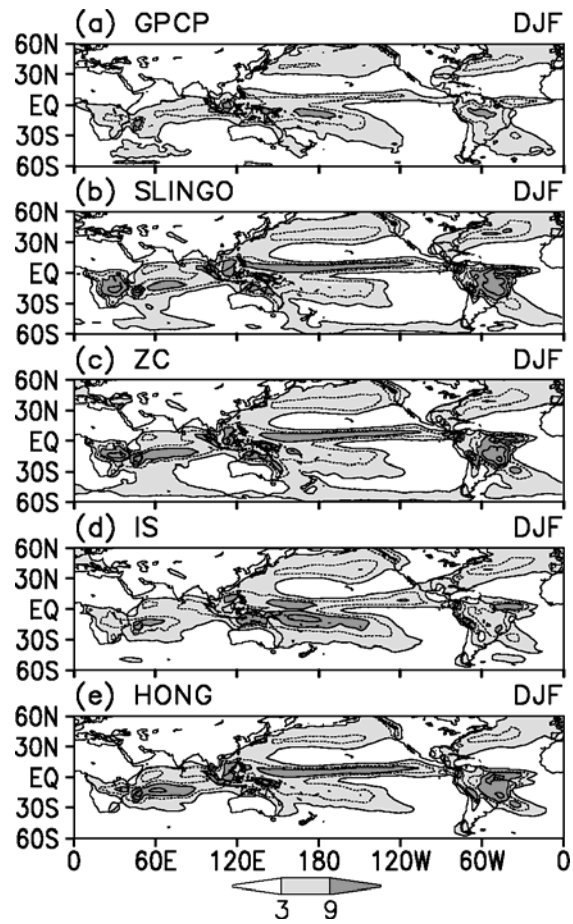


Fig.7 As in Fig.3, but for precipitation (mm day^{-1}) in DJF. (a) GPCP observed, (b) SLINGO, (c) ZC, (d) IS and (e) HONG are displayed. Contour lines are 3, 9, 15, and 21 mm day^{-1} . Light stippled area is for between 3 and 9 and heavy stippled for above 9 mm day^{-1} .

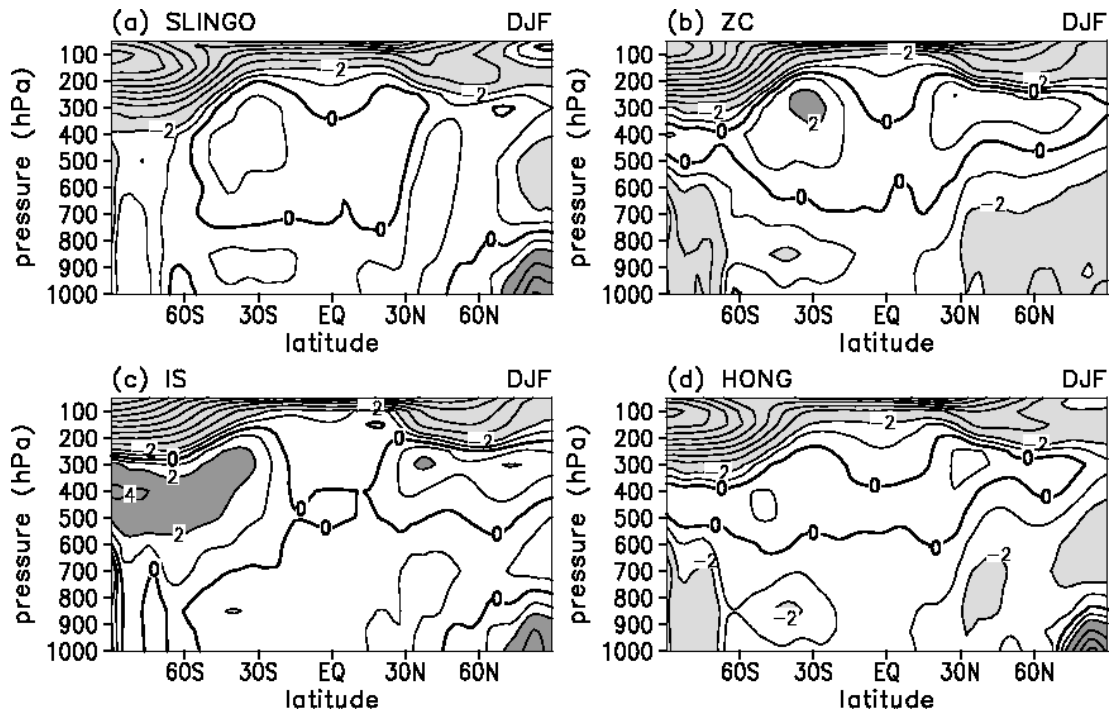


Fig.8 Zonally averaged temperature differences ($^{\circ}\text{K}$) from R-2 for (a) SLINGO, (b) ZC, (c) IS and (d) HONG in DJF for 1990 – 1999. Contour indicates $\pm 1^{\circ}\text{K}$ and then every 2°K . Area of light stippling is for below -2 and heavy stippling is for above 2 .

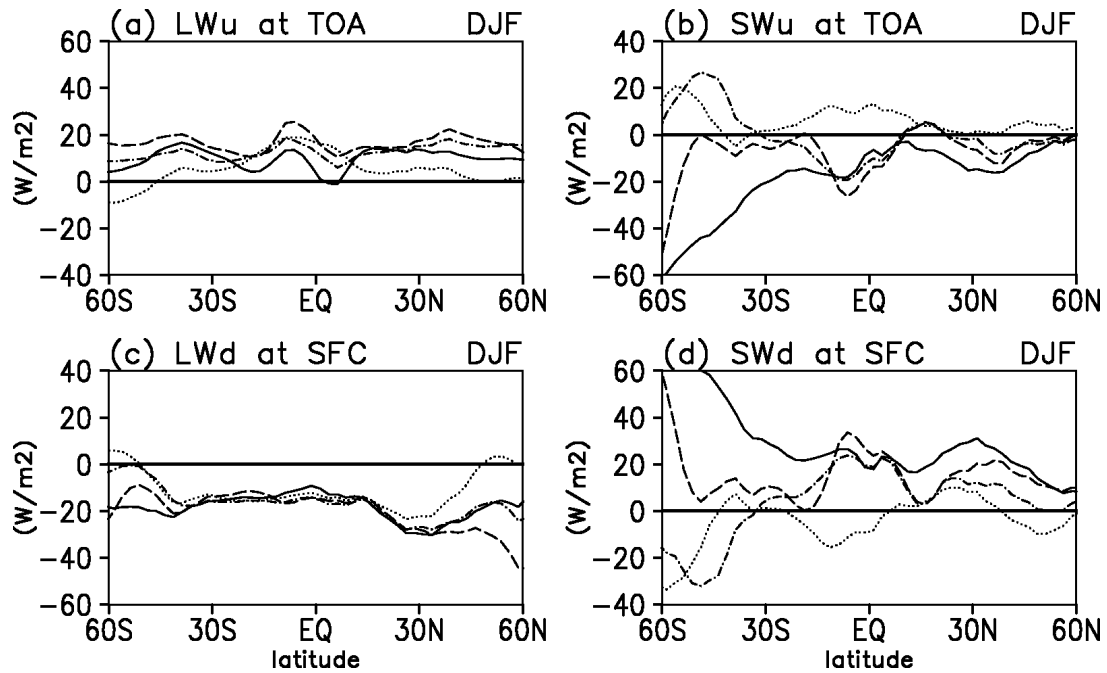


Fig.9 Differences of zonally averaged radiation fluxes between simulation and observation in DJF. (a) upward longwave radiation flux at TOA, (b) upward shortwave radiation flux at TOA, (c) downward longwave radiation flux at SFC and (d) downward shortwave radiation flux at SFC. Observed radiation fluxes are from ERBE for TOA and SRB for SFC. The period of observation is 1990-1999 for SRB and 1985-1989 for ERBE. Unit is in $W m^{-2}$.

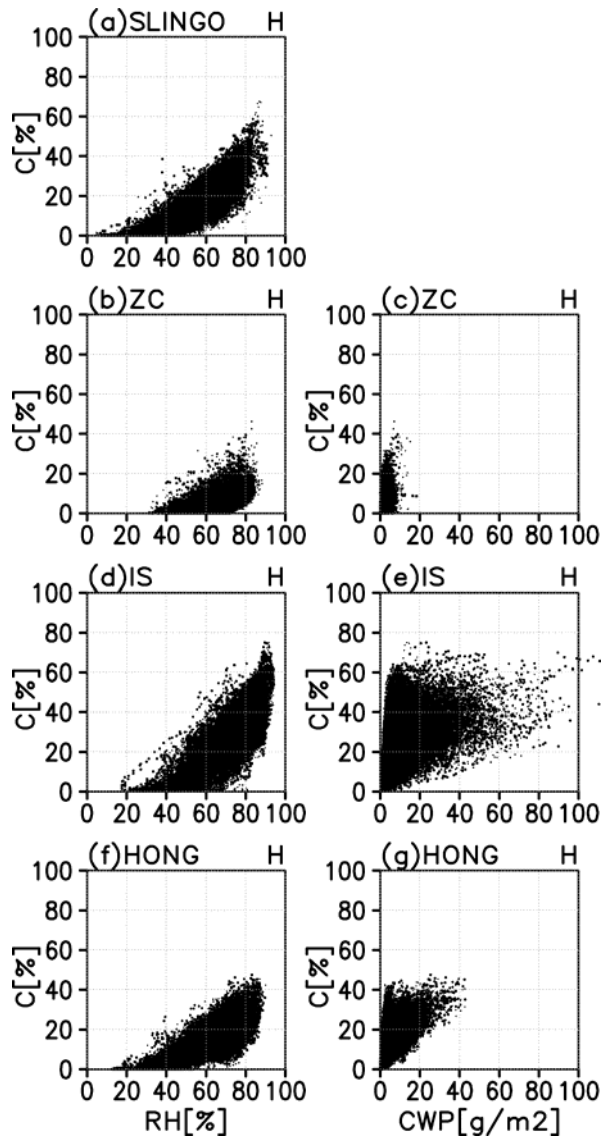


Fig. 10 Scatter diagrams of relative humidity vs. cloud amount (left panels) and cloud water path vs. cloud amount (right panels) for high cloud from SLINGO (a), ZC (b and c), IS (d and e) and HONG (f and g) simulations over the area [0-360, 30°N-60°N] during January 1999 – December 1999. Units of relative humidity and cloud amount are in percent and cloud water path in g m^{-2} .

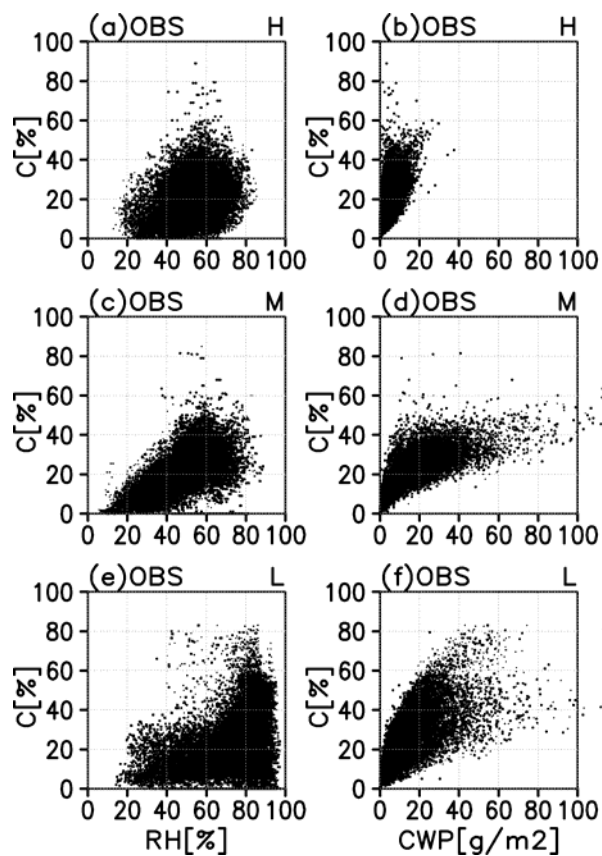


Fig. 11 Scatter diagrams of relative humidity vs. cloud amount (left panels) and cloud water path vs. cloud amount (right panels) for high (a and b), middle (c and d) and low clouds (g and h) from observation (ISCCP) and reanalysis (R-2) over the area [0-360, 30°N-60°N] during January 1999 – December 1999. Units of relative humidity and cloud amount are in percent and cloud water path in g m^{-2} .

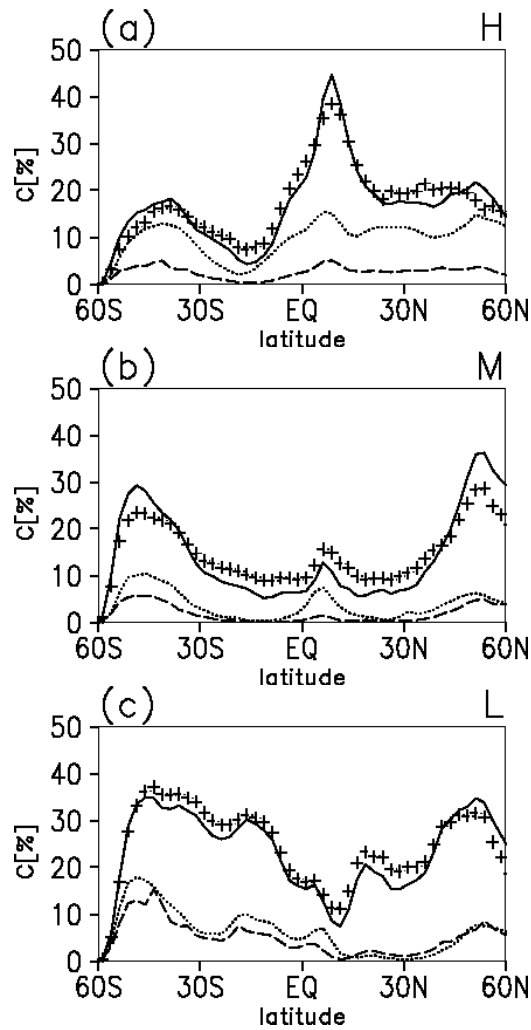


Fig. 12 Monthly averaged zonal mean cloud amount (%) from ISCCP observation (cross marks), cloud amount calculated from relative humidity only based on Slingo (1987) (dotted line), calculated from relative humidity and cloud water based on Randall (1995) (dashed line) and calculated from cloud water only based on new formula (solid line). (a) High, (b) middle and (c) low clouds for July 2000 are shown. For the calculation, 6 hourly cloud water from ISCCP D1 data and relative humidity from R-2 were used.